BMC Veterinary Research

RESEARCH

Open Access

# Identification and characterization of pigeon adenovirus 1 as an emerging pathogen in pigeons from Northern and Northwest China

Zhiyuan Yang[1†], Yuting Zhou[1†], Jian Lin[1†], Xiuqing Wang[3], Cheng Huang[1], Jie Gao[2], Guoliang Wang[4], Baolin Yang[1], Guiming Liu[4], Huijuan Duan[1], Jian Cui[1], Jicheng Zhao[1], Weijue Luo[2], Shuisheng Cheng[2*] and Yuehuan Liu[1*]

## Abstract

**Background** In 2022, a new infectious disease characterized by severe acute hepatitis, sudden death, and high mortality among breeding pigeons, was reported in China.

**Results** In naturally infected pigeons, key necropsy findings comprised hepatic swelling with patchy hemorrhage and pericardial effusion. Histopathological examination further revealed degeneration, necrosis, and basophilic intranuclear inclusion bodies affecting hepatocytes, cardiomyocytes, and vascular endothelial cells. Transmission electron microscopy revealed a typical icosahedral virus structure and crystal-like arrangement of viral particles in the nucleus. Metagenomic next-generation sequencing (mNGS) of pericardial effusion samples revealed the presence of pigeon adenovirus. Sequencing analysis of the *hexon* and *fiber-2* genes suggested that it constituted pigeon adenovirus 1 (PiAdV-1). The complete genome of CH/BJ/1/2022 was determined to be 48,071 nucleotides in length, with a 10-amino acid deletion in the *fiber-2* gene at residues 627–636 and a 95-animo acid insertion in the 100 K gene at residue 75. The same disease was reproduced in pigeons by experimental infection.

**Conclusion** Collectively, our analyses confirmed that the etiological agent was PiAdV-1, an emerging pathogen that causes severe acute hepatitis and high mortality in pigeons. This virus merits close attention because it could be catastrophic for the pigeon industry.

**Keywords** Pigeon adenovirus 1, PiAdV-1, Fiber-2, Pigeon, Pathological changes, Viral characterization

†Zhiyuan Yang, Yuting Zhou and Jian Lin contributed equally to this work.

*Correspondence:
Shuisheng Cheng
1926691773@qq.com
Yuehuan Liu
liuyuehuan@sina.com

[1]Institute of Animal Husbandry and Veterinary Medicine, Beijing Academy of Agriculture and Forestry Sciences, No. 9 Shuguang Garden Middle Road, Haidian District, Beijing 100097, P. R. China
[2]Beijing Zhonghai Biotech, Co., Ltd., Beijing 100081, China
[3]South Dakota State University, Brookings, SD 57007, USA
[4]Institute of Biotechnology, Beijing Academy of Agriculture and Forestry Sciences, Beijing 100097, China

## Background

Domestic pigeons, which belong to the family *Columbidae*, have important roles in nature and human life. They are used for racing because of their majestic flight, for ornamental purposes because of their attractive appearance, and for meals because of their nutritious meat. Numerous viral infections (e.g., involving paramyxoviruses, circoviruses, rotaviruses, herpesviruses, poxviruses, and adenoviruses) are major problems for the meat and racing pigeon industries [1]. The most important disease, paramyxovirus type I infection, is responsible for high morbidity and mortality in pigeons.

Adenoviruses, members of the family *Adenoviridae* [2], are non-enveloped viruses with double-stranded DNA and genomes of approximately 38 to 45 kb, which encode several nonstructural proteins, as well as three major structural proteins: hexon, fiber, and penton base [3, 4]. The *Adenoviridae* family is subdivided into six genera, *Aviadenovirus*, *Barthadenovirus*, *Ichtadenovirus*, *Mastadenovirus*, *Siadenovirus*, and *Testadenovirus*. The genus *Aviadenovirus* comprises 16 species, including *Fowl aviadenovirus* (FAdV) *A-E*, *Pigeon aviadenovirus* (PiAdV) *A-B*, *Turkey aviadenovirus* (TAdV) *B-D*, *Psittacine aviadenovirus* (PsAdV) *B-C*, *Falcon aviadenovirus* (FaAdV) *A*, *Duck aviadenovirus* (DAdV) *B*, *Goose aviadenovirus* (GoAdV) *A*, and *Aviadenovirus leucophthalmi* ( https://ictv.global/report/adenoviridae). Aviadenovirus are widely distributed in chickens, turkeys, pigeons, parrots, ducks, and other avian species [5].

Adenoviral infection in pigeons was firstly described in 1976 [6] and has since been observed worldwide [7]. Natural adenoviral infection of pigeons is caused by pigeon adenovirus 1 (PiAdV-1, classified under *Pigeon aviadenovirus A*) [8, 9], pigeon adenovirus 2 (PiAdV-2, classified under *Pigeon aviadenovirus B*) [10, 11], and specific serotypes of fowl adenoviruses (FAdV) [12, 13]. Pigeon adenoviruses are known to cause two types of clinical diseases: classical adenovirosis and necrotizing hepatitis [7]. Classical adenovirosis, which mainly occurs in pigeons aged < 1 year, is characterized by catarrhal enteritis [14]. Necrotizing hepatitis causes extensive hepatic necrosis and results in sudden death among pigeons [7, 15, 16]. The annual pigeon mortality rate is notably high, with approximately 30% attributed to PiAdV infection. In some cases, however, it can reach 100% in pigeon lofts affected by necrotizing hepatitis [7].

From February 2022 through 2024, an infectious disease characterized by the sudden death of breeding pigeons was observed on many racing pigeon and meat pigeon farms in Beijing, Tianjin, Hebei, Shanxi, Shaanxi, Inner Mongolia, Xinjiang, and other major pigeon breeding regions in China. The disease caused significant economic losses to the pigeon industry in China. Here, we used affected pigeons to perform a systematic investigation that included epidemiology, gross pathological and histopathological analyses, metagenomic next-generation sequencing (mNGS), pathogen isolation, genome sequencing, and animal experiments. We found that the etiological agent of the disease causing high mortality among breeding pigeons was pigeon adenovirus 1 (PiAdV-1).

## Results

### Epidemiological investigation

Since October 2022, a serious and suddenly emerging epidemic of pigeon adenovirus disease, characterized by diffuse hepatic necrosis and sudden death, has been observed in racing pigeon and meat pigeon farms across Beijing, Tianjin, Hebei, Shanxi, Shaanxi, Inner Mongolia, Xinjiang, and other major pigeon breeding regions in China.

On meat pigeon farms, the disease spread slowly among pigeon houses, with low daily mortality. Affected breeding pigeons exhibited weight loss and sudden death, leading to a cumulative mortality rate of 15% and significant economic losses. On racing pigeon farms, the disease primarily affected pigeons aged 5–6 months, causing reduced food intake, emaciation, and a mortality rate of 10–13%, severely impacting their competitiveness.

Among 125 liver tissue samples collected from 10 different farms in Northern and Northwest China, 108 (86.4%) were positive for PiAdV-1 by PCR (Table 1), while all were negative for PiAdV-2 and FAdV-C (Table S4). Serum samples collected from seven provinces in Northern and Northwest China from October 2022 to July 2024 were also analyzed. Among 250 serum samples, 156 (62.4%) were positive for adenovirus antibody by ELISA (Table 1). Serological surveillance revealed a year-on-year increase in seroprevalence, with antibody positivity rates for adenovirus rising from 8.4% (7/83) in 2021 to 45.7% (32/70) in 2022, 67.1% (53/79) in 2023, and 73.9% (51/69) in 2024 (Table S2). Since vaccine against PiAdVs is not currently available in China, the detected antibodies in these birds could only be due to natural infection. These findings indicated that PiAdV infections have been widespread in China in recent years.

### Pathological findings

In naturally infected pigeons, common gross pathological findings included breast discoloration (Supplementary Fig. 3A). The liver was swollen, yellowish, and fragile (Fig. 1A). Black and poorly clotting blood was observed in the liver, heart, and other organs (Fig. 1B). Hydropericardium and heart discoloration were also observed (Fig. 1C). Finally, renal swelling (Supplementary Fig. 3B), splenic swelling (Supplementary Fig. 3C), and egg follicles with patchy hemorrhage (Supplementary Fig. 3D) were present.

**Table 1** Seroprevalence and molecular detection of pigeon adenovirus (PiAdV) in pigeons from different regions of China

| No. | Region | Sampling Site | Species | Approx. stock | Collection Date | Positive samples by PCR, *n*/Tissue samples tested, *n* (Positivity %) | Positive samples by ELISA, *n*/Serum samples tested, *n* (Positivity %) |
|---|---|---|---|---|---|---|---|
| 1 | Beijing | 1 | Meat Pigeon | 20,000 pairs | 2022-10-21 | 31/34 (91.1) | 15/40 (37.5) |
| | | 2 | Meat Pigeon | 100,000 pairs | 2023-01-08 | 25/28 (89.3) | 29/39 (74.4) |
| | | 3 | Meat Pigeon | 20,000 pairs | 2023-02-02 | N/A | 12/20 (60.0) |
| | | 4 | Meat Pigeon | 2,000 pairs | 2024-05-24 | N/A | 33/40 (82.5) |
| 2 | Tianjin | 1 | Racing pigeon | 10,000 | 2024-07-25 | N/A | 20/32 (62.5) |
| 3 | Hebei | 1 | Racing pigeon | 15,000 | 2022-04-06 | N/A | 17/30 (56.7) |
| | | 2 | Racing pigeon | 10,000 | 2023-02-06 | 4/10 (40.0) | N/A |
| | | 3 | Racing pigeon | 10,000 | 2023-07-21 | 7/7 (100) | N/A |
| | | 4 | Racing pigeon | 10,000 | 2024-03-09 | 4/4 (100) | 7/10 (70.0) |
| 4 | Shanxi | 1 | Racing pigeon | 12,000 | 2023-07-04 | 18/19 (94.7) | 9/10 (90.0) |
| 5 | Shaanxi | 1 | Racing pigeon | 10,000 | 2023-07-10 | 7/7 (100) | N/A |
| 6 | Inner Mongolia | 1 | Racing pigeon | 8,000 | 2023-07-27 | 9/9 (100) | 3/10 (30.0) |
| | | 2 | Racing pigeon | 10,000 | 2024-07-28 | 1/3 (33.3) | 11/19 (57.9) |
| 7 | Xinjiang | 1 | Racing pigeon | 5,000 | 2022-12-27 | 2/4 (50.0) | N/A |
| | Total | 15 | / | / | / | 108/125 (86.4) | 156/250 (62.4) |

Infiltrating lymphocytes and macrophages were observed in hepatic portal areas. Disseminated fat degeneration and focal areas of necrosis were observed throughout the liver. Hepatocytes also contained basophilic intranuclear inclusion bodies (Fig. 1D). Degeneration, necrosis, endothelial cell loss, and the presence of basophilic intranuclear inclusion bodies were observed in endothelial cells (Fig. 1E). Severe degeneration and necrosis of bile duct epithelial cells, infiltration of inflammatory cells, and bile acid salt deposition were also observed (Supplementary Fig. 3F). Swollen, degenerated, and necrotic cardiomyocytes were present, along with degenerated and necrotic endothelial cells near cardiomyocytes with suspected basophilic intranuclear inclusion bodies (Fig. 1F). Cardiomyocytes lost their striated appearance and became disorganized (Fig. 1F). The lower parts of the jejunum, ileum, cecum, and rectum appeared normal. Granular denaturation, vacuolar degeneration, basophilic inclusion bodies, and necrosis were observed in renal tubular epithelial cells (Fig. 1G). Furthermore, degenerated and necrotic endothelial cells were visible. Congestion, edema, and inflammatory cell infiltrates were identified (Supplementary Fig. 3G). Splenic white pulp displayed a substantial decrease in lymphocyte number. The white pulp was reduced in size and had been infiltrated by numerous reticular cells and macrophages; some of these cells contained basophilic intranuclear inclusion bodies (Fig. 1H). Degeneration, necrosis, and shedding of duodenal epithelial cells and the upper part of jejunal epithelial cells were evident, along with basophilic intranuclear inclusion bodies in those cells (Fig. 1I). The histological results were consistently observed across multiple pigeons, representing collective manifestations. Notably, basophilic intranuclear inclusion bodies in hepatocytes were prevalent among all examined pigeons, and similar features like inflammatory cell infiltrates were seen in various organs, suggesting a common cause. Fibrous tissue in pectoral muscle of a few pigeons became disorganized (Supplementary Fig. 3E). Brain, spinal cord, lungs, esophagus, and glandular stomach appeared normal.

#### Ultrastructural findings

Swollen mitochondria and mitochondrial cristae rupture were observed in hepatocytes, along with endoplasmic reticulum expansion. TEM revealed numerous viral particles in the nucleus of an infected hepatocyte (Fig. 2A). Ultrathin sections showed scattered and lattice (crystal-like structure) (Fig. 2B) arrangements of icosahedral viral particles (approximately 70–90 nm; Fig. 2C and D) in the nuclei of infected hepatocytes; these particles appeared similar to adenovirus.

#### mNGS sequence characteristics

The read counts can roughly indicate the relative infection levels in different samples. After the exclusion of host reads, the most abundant viral pathogen in the five pericardial effusion samples was PiAdV-1, with the following numbers of reads detected: 18,014, 64,048, 1363, 14,501, and 467,985 (Table 2), suggesting widespread presence and high abundance. In contrast, Pigeon adenovirus 2 is scarcely detected with only 1 read in A3. Other viruses like Valbvirus ValB1MD2 with some read counts are less common pathogens in pigeons.

#### Sequence alignment and phylogenetic analysis

As shown in Fig. 3A, PCR products with expected sizes of 3064 bp for *hexon* gene and 2678 bp for *fiber-2* gene were

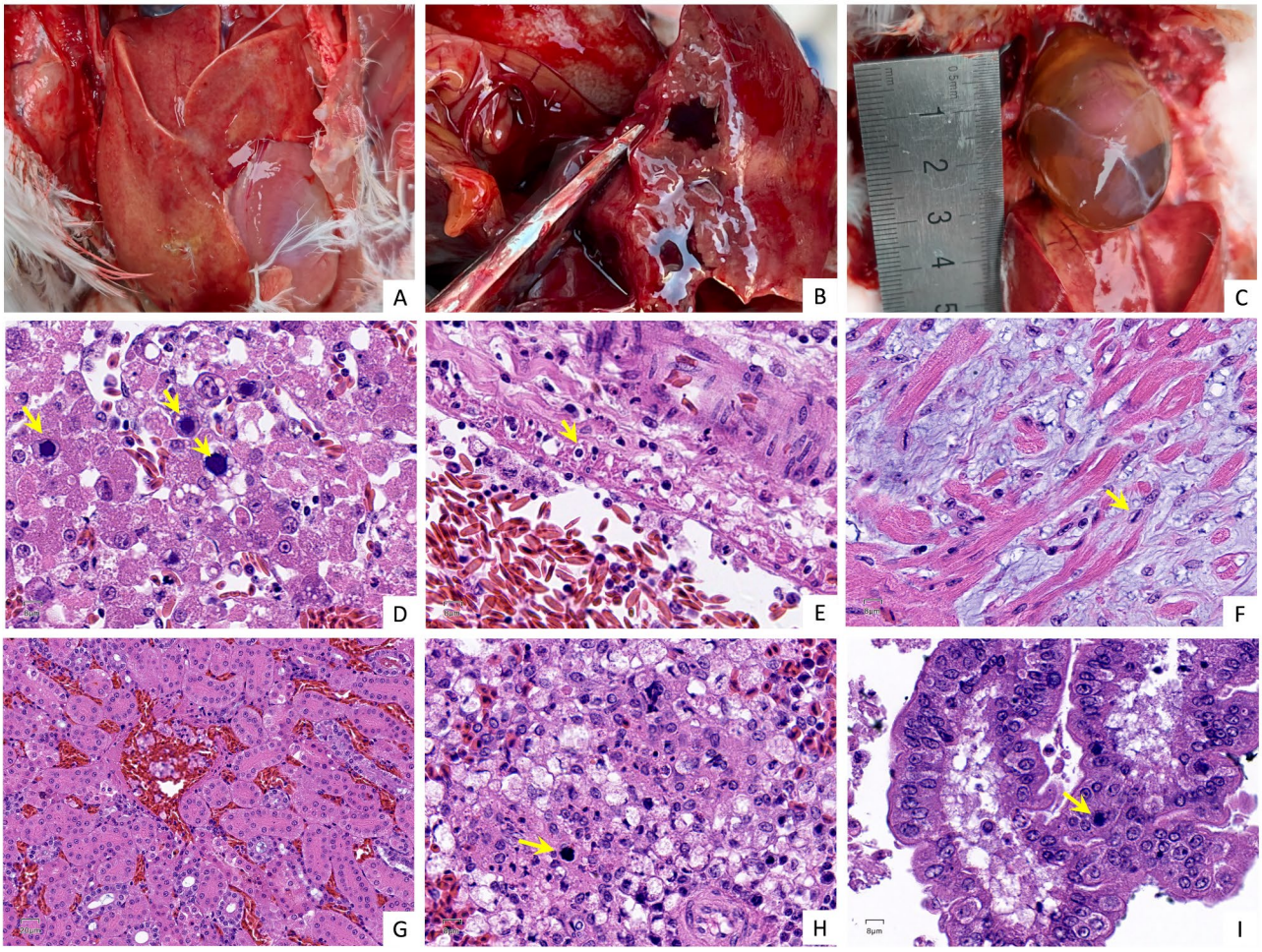


**Fig. 1** Pathological features of PiAdV-1-infected pigeons. (**A-D**) Gross pathology: (**A**) Hepatic swelling with multifocal hemorrhages and capsular fragility. (**B**) Intrahepatic unclotted blood (black arrows) indicative of coagulopathy. (**C**) Hydropericardium and myocardial discoloration. (**D-I**) Histopathology (H&E staining): (**D**) Liver: Hepatocellular necrosis and basophilic intranuclear inclusion bodies. (**E**) Liver: Necrotic vascular endothelium. (**F**) Heart: Cardiomyocyte degeneration. (**G**) Kidney: Tubular epithelial necrosis. (**H**) Spleen: Lymphocyte depletion. (**I**) Jejunum: Villous epithelial necrosis. Yellow arrows indicate basophilic intranuclear inclusion bodies in the nuclei of infected cells

amplified from DNA extracted from positive samples collected in Beijing, Hebei, Xinjiang, Shanxi, Shaanxi, and, Inner Mongolia. The six new isolates were designated as CH/BJ/1/2022, CH/HB/1/2022, CH/XJ/1/2022, CH/Shaanxi/1/2023, CH/SX/1/2023, and CH/NMG/1/2023. DNA sequencing of the purified PCR products indicated that both the *hexon* and *fiber-2* genes shared a high sequence identity of 99% among all isolates. BLAST searches revealed that the *hexon* and *fiber-2* genes showed respective pairwise sequence identities of 99.48% and 97.07% (at the amino acid level) with the IDA4 strain of PiAdV-1 [9]. Phylogenetic analysis confirmed that all six isolates were classified as *Pigeon aviadenovirus A* (Fig. 3B and C). Furthermore, the *fiber-2* gene of the CH/BJ/1/2022 strain exhibited 98.18–98.71% nucleotide similarity to other PiAdV-1 strains (P18-05523-6, TR/SKPA20, and pAd-4) from Australia, Turkey, and Iran, as previously reported in GenBank (Table 3). The analyzed datasets were submitted to the NCBI GenBank database under the following accession numbers: OQ451133, OQ451134, OQ576011- OQ576014, PP495492-PP495494, and PP495496-PP495498.

### Genome properties of the isolates

The whole genome nucleotide sequence of CH/BJ/1/2022 is available in the GenBank database under accession number PP495491. The complete genome of CH/BJ/1/2022 was found to be 45,817 base pairs (bp) in length, and a G + C content of 64%. The percent sequence identity of strain CH/BJ/1/2022 showed the highest sequence homology (98.35%) with strain IDA4 (PiAdV-1, Accession: NC_024474.1), which was isolated in the Netherland at nucleotide level. In contrast, it exhibited a lower sequence identity (56.66%) with isolate YPDS-Y-V1.A19.11-2013 (PiAdV-B, Accession: NC_031503.1). Similar to strain IDA4, the inverted terminal repeat

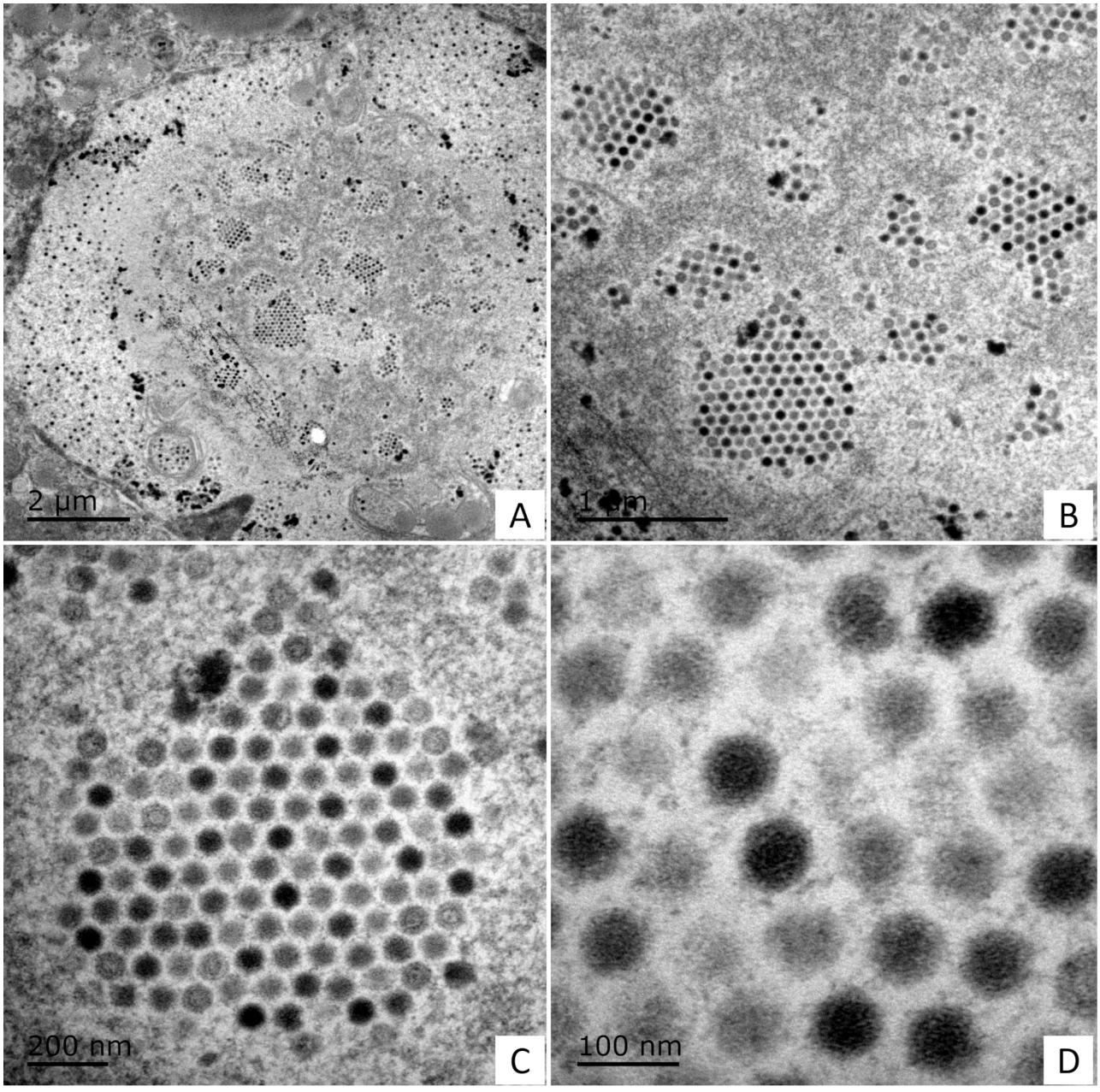


**Fig. 2** Transmission electron microscopy images of pigeon adenovirus viral particles in the nucleus of an infected hepatocyte. Virions were arranged in the form of a lattice (**A & B**) and exhibited a diameter of 70–90 nm (**C & D**)

(ITR) sequences of strain CH/BJ/1/2022 was found to be 45 bp long. The open reading frames (ORFs) and terminal regions of the genomic sequence were almost identical to those of strain IDA4, comprising 33 potential ORFs (Fig. 4). To investigate the mutation profile, we analyzed and compared the complete genome sequences of CH/BJ/1/2022 with those of two other PiAdV-1 strains, IDA4 (NC_024474.1) and P18-05523-6 (MW286325.1). The results showed that the isolate in the present study had a 10-amino acid deletion in the *fiber-2* gene at residues 627–636 and a 95-amino acid insertion in the 100 K gene (encoding hexon assembly protein 100 K) at residue 75, based on the numbering of IDA4 (NC 024474.1).

### Virus isolation

Pigeon embryos inoculated with supernatants of homogenized livers were all dead at 136–144 h post-inoculation. Dead pigeon embryos with hemorrhage and enlarged liver (Fig. 5) were observed in three successive experiments. The *hexon* gene of PiAdV-1 was present in DNA extracted from the supernatants of dead pigeon embryos. Nevertheless, all inoculated specific pathogen-free

**Table 2** Number of mNGS reads in pericardial effusion samples

| Pathogenic microorganism | Number of mNGS reads in pericardial effusions[a] | | | | |
|---|---|---|---|---|---|
| | A 1 | A 2 | A 3 | Y 1 | Y 2 |
| Pigeon adenovirus 1 | 28,240 | 73,138 | 61,819 | 74,205 | 477,841 |
| Pigeon adenovirus 2 | / | / | 1 | / | / |
| Valbvirus ValB1MD2 | 2246 | 2239 | 20,901 | 22,596 | 2994 |
| Pigeonpox virus | / | 3 | 1 | 1 | / |
| Avian orthoavulavirus 1 | / | 1 | / | 3 | 2 |
| Mycobacterium canettii | 72,957 | 58,783 | 498,308 | 357,505 | 140,693 |
| Klebsiella pneumoniae | 24,746 | 20,594 | 49,639 | 68,082 | 79,078 |
| Escherichia coli | 14,156 | 8606 | 15,767 | 14,330 | 820 |

[a]A1–A3 were adult pigeons, Y1–Y2 were young pigeons

chicken embryos remained alive; PCR analysis revealed that none of these embryos contained DNA encoding the *hexon* gene of PiAdV-1.

### Experimental infection of pigeons

Two of five PiAdV-1-inoculated pigeons developed clinical signs of fluffy feathers and depression beginning at 4 dpi. These two pigeons died at 6 dpi; they exhibited significant liver enlargement and patchy hemorrhage in the liver (Fig. 6A and B). The other three infected pigeons were euthanized at 8 dpi for histopathology analysis. Gross pathological findings included hepatic and renal swelling. Histopathological findings included diffuse liver necrosis, as well as basophilic and eosinophilic inclusion bodies in the nuclei of hepatocytes (Fig. 6D and E) and renal tubular epithelial cells. PCR revealed successful amplification of viral DNA from the five infected pigeons; subsequent isolation of the virus satisfied Koch's postulates. No control pigeons showed pathological changes (Fig. 6C and F), and samples from those pigeons did not contain viral DNA. As shown in Fig. 7, all serum samples from infected pigeons contained antibodies against adenoviruses, and ELISA showed a significant increase in antibody level at 8 dpi ($p < 0.01$).

## Discussion

Over the past decades, adenovirus infections in chicken, ducks, pigeons and quails have become increasingly complex, causing severe economic losses within the poultry industries of China, India, the United States, Canada, and several European countries [17–21]. The sudden increase in mortality among breeding pigeons on racing and meat farms in Northern and Northwest China has led to significant economic losses in the pigeon industry.

Pigeon adenovirus infections can easily be diagnosed by the presence of basophilic intranuclear inclusion bodies in hepatocytes, as well as the characteristic lattice arrangement of icosahedral viral particles in the nuclei of infected cells [7, 22]. While PCR is widely used for screening adenovirus in chickens, pigeons, and parrots [11, 23–26]. Sequencing of the *hexon* and *fiber-2* genes is essential for precise typing. Through this approach, we identified six new isolates (CH/BJ/1/2022, CH/HB/1/2022, CH/XJ/1/2022, CH/SX/1/2023, CH/Shaanxi/1/2023, and CH/NMG/1/2023) from deceased pigeons in Northern and Northwest China, confirming PiAdV-1 as the causative pathogen. Clinically, both PiAdV-1 and PiAdV-2 have been reported in China [11, 27], but their roles in specific diseases remain unclear and are often confused. PiAdV-2 is frequently carried asymptomatically in healthy pigeons [28], and co-infections with PiAdV-1 may occur [27], though none were detected in this study. Critically, PiAdV-1 and PiAdV-2 exhibit significant genetic divergence, particularly in the *fiber-2* gene (sequence similarity < 52.7%) [10]. This low similarity suggests substantial antigenic differences, necessitating separate vaccine development for each type.

To date, PiAdV-1 infections in pigeons have been reported worldwide [9, 27, 29, 30]. Studies in Turkey and Australia documented PiAdV-1 co-infections with PiCV [30] or torque teno virus (PTTV) [9], respectively, both presenting severe hepatic necrosis and intranuclear inclusions. In contrast, Iranian surveys reported low PiAdV-1 prevalence (4.16%) in both healthy and diseased pigeons [29], suggesting regional differences in pathogenicity. In this study, we confirmed the presentation of adenoviral particles in the nucleus of infected hepatocytes by TEM. In addition, we observed multiple basophilic intranuclear inclusion bodies in cardiomyocytes and endothelial cells. Similarly, Li et al. [27]described PiAdV-1-induced fulminant hepatitis with hepatic necrosis and renal damage but did not report cardiac or endothelial involvement. These findings align with classical adenovirosis type II, characterized by sudden death and fulminant hepatitis. Combined with emerging reports of PiAdV-1 outbreaks in China, our findings highlight a trend toward heightened pathogenicity, necessitating vigilance in pigeon industry.

A retrospective serological analysis revealed the presence of antibodies to pigeon adenovirus among pigeons in different regions of China in 2021, with significant increases in antibody positivity in 2022, 2023, and 2024. In this study, the Fowl Adenovirus Group 1 Antibody

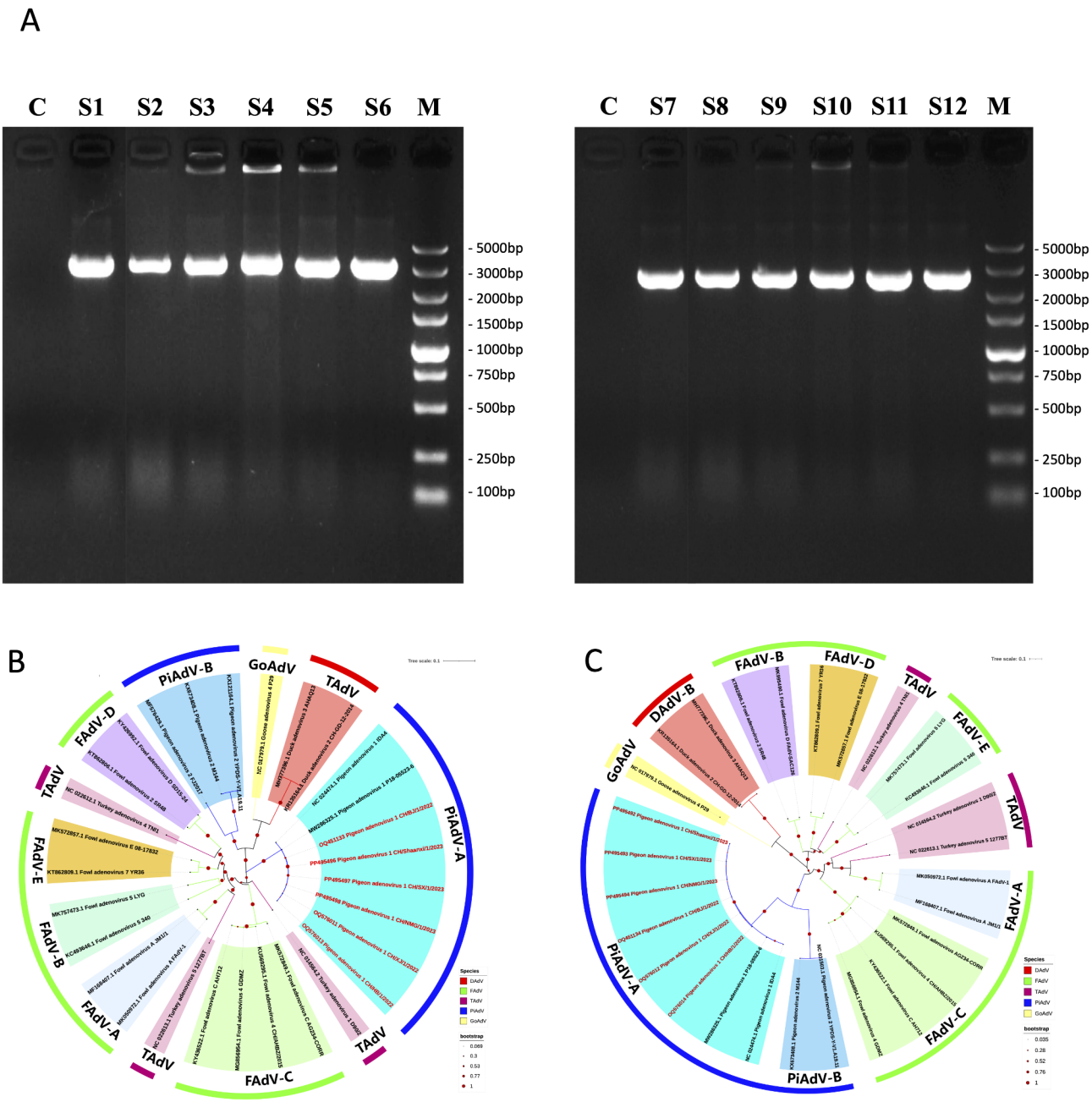


**Fig. 3** Molecular characterization of pigeon adenovirus. (**A**) Agarose gel showing the results of PCR with primers specific for the *hexon* and *fiber-2* genes of PiAdV-1. S1–S6: pigeon liver supernatants collected from Beijing, Hebei, Xinjiang, Shanxi, Shaanxi, and, Inner Mongolia were subjected to *hexon* gene amplification, and the band is located at approximately 3064 bp; S7–S12: pigeon liver supernatants collected from Beijing, Hebei, Xinjiang, Shanxi, Shaanxi, and, Inner Mongolia were subjected to *fiber-2* gene amplification, and the band is located at approximately 2678 bp; C: negative control; M: DL5000 bp ladder marker. For consistency in presentation, 'S1' and the negative control were cropped, reordered, and stitched with 'S2-S6'. Similarly, 'S7' and the negative control were cropped, reordered, and stitched with 'S8-S12'. The full-length gel for the left panel is presented in Supplementary Fig. 1, and for the right panel in Supplementary Fig. 2. (**B**) Phylogenetic tree based on alignment of sequenced *hexon* gene PCR products with reference avian adenovirus strains. (**C**) Phylogenetic tree based on alignment of sequenced *fiber-2* gene PCR products with reference avian adenovirus strains. Trees were generated using the neighbor-joining method, coupled with the Kimura 2-parameter model and bootstrap analysis of 1000 replicates. In (**B**) and (**C**), the five colors (red, green, magenta, blue and light yellow) of the outer ring sequentially represent the five species of *Aviadenoviruses*: DAdV, FAdV, TAdV, PiAdV, and GoAdV, while the different background colors in the inner circle represent distinct clades. Trees show the name and GenBank accession number of each isolate, and the six strains highlighted in red font were obtained in this study

**Table 3** Nucleotide sequence identity (%) of the *Hexon* and *fiber-2* genes of CH/BJ/1/2022 strain compared with the previously identified PiAdV-1 strains

| Strain | Country | Accession | Identity with CH/BJ/1/2022 | |
|---|---|---|---|---|
| | | | hexon | fiber-2 |
| IDA4 | Netherlands | NC_024474.1 | 99.51% | 98.39% |
| P18-05523-6 | Australia | MW286325.1 | 99.62% | 98.18% |
| TR/SKPA20 | Turkey | MN985817.1 | N/A | 98.28% |
| pAd-4 | Iran | OL538251.1 | N/A | 98.71% |

N/A: *hexon* gene sequence not available

test kit (BioChek Ltd.) was utilized, its chicken-specific design poses limitations due to cross-reactivity differences between avian species. To address this, we compared the original protocol (anti-chicken secondary antibody) with a modified version using rabbit anti-pigeon IgY Secondary antibody (HRP) and TMB system, achieving a concordance rate of 84.4% (Table S5), confirming reasonable reliability. In addition, false positives may occur as a result of the cross-reactivity among the multiple serotypes of FAdV Group 1 [31]. Despite this, previous reports [28] and our current survey indicate that, to date, PiAdV-1 and PiAdV-2 are the primary adenovirus species infecting pigeons in China, with relatively few reports of other FAdV infections [23]. Consequently, the observed increase in antibody positive rates strongly suggests a growing prevalence of pigeon adenovirus infections. To validate these findings and improve surveillance accuracy, developing pigeon-specific serological assays is imperative.

Unlike most aviadenoviruses, which are not always directly associated with overt clinical disease [23, 32], pigeon adenoviruses are often highly virulent and directly cause clinical disease in infected birds. Pigeon adenovirus infections occur worldwide and can cause significant economic losses [7]. In the past decade, pigeon adenovirus infections have been reported in Australia, China, and other countries [9–11, 25]. Pigeons infected with adenovirus are associated with two clinical types: classical adenovirosis and necrotizing hepatitis [7]. Notably, we observed both necrotizing hepatitis and enteritis in necropsied pigeons. Additionally, we encountered hydropericardium, along with degenerated and necrotic cardiomyocytes, endothelial cells, and renal tubular epithelial cells. Hepatitis-hydropericardium syndrome has been reported as a result of aviadenovirus infection in chickens, ducks, and wild birds [33]. Canine adenovirus type I exhibits tissue tropism for both hepatocytes and vascular endothelial cells, leading to systemic infections that involve multiple organs (e.g., kidney, heart, and spleen) [34]. We have observed similar systemic manifestations in pigeons. Our findings demonstrate the broad organ tropism of PiAdV-1. Histopathological evidence confirms significant viral proliferation and inflammatory damage in both liver and kidney tissues. The characteristic gross pathological and histopathological findings in the present pigeon adenovirus disease are similar to those of a typical adenoviral infection.

Pigeon adenovirus and circovirus co-infection was recently identified in a flock of pigeons with young pigeon disease syndrome in Turkey [30]. A recent study in Australia showed that both PiAdV-1 virus and pigeon torque teno virus were present in an outbreak of necrotizing hepatitis [9]. The results of an epidemiological survey in Poland suggest that, compared with pigeon adenoviruses, pigeon circoviruses and pigeon herpesviruses more commonly cause young pigeon disease syndrome [14]. Similar findings regarding circovirus infections in pigeons were reported in China [35]. In cases of pigeon herpesvirus infection, hepatocytes typically exhibit eosinophilic inclusion bodies [36]. Pigeon circoviruses display tissue tropism for the bursa [37]. In the present study, although eosinophilic inclusion bodies were observed in the infected cells of field-collected liver samples, PCR analysis of these liver samples failed to detect herpesvirus. In contrast, circovirus was present in liver and spleen tissue samples (Table S4). However, we suspect that pigeon circovirus was not the etiological agent of the disease present among the naturally infected pigeons in the present study, based on the gross pathological and histopathological findings. Furthermore, we performed mNGS to

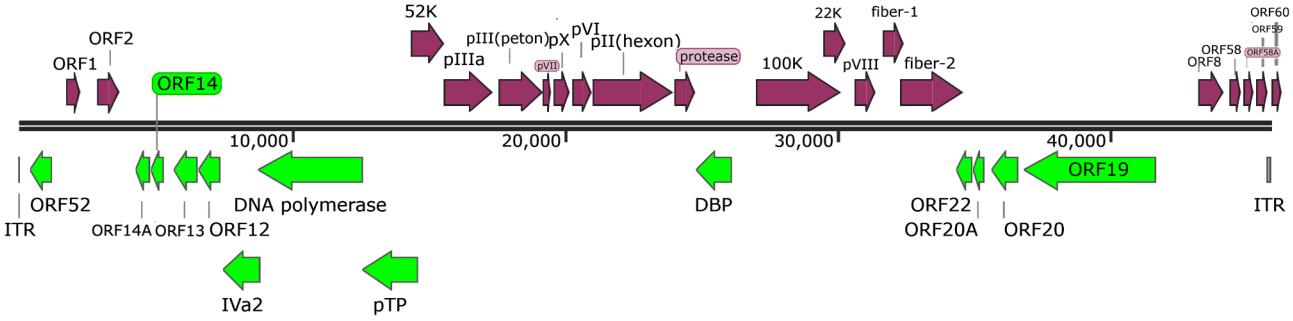


**Fig. 4** Schematic illustration of genome organization of the isolate CH/BJ/1/2022. Two lines indicates DNA strands. Numbers at the bottom show base pairs (BP). The arrows denote the predicted proteins, labeled by protein name. Orientation of the arrows indicates the direction of transcription/translation

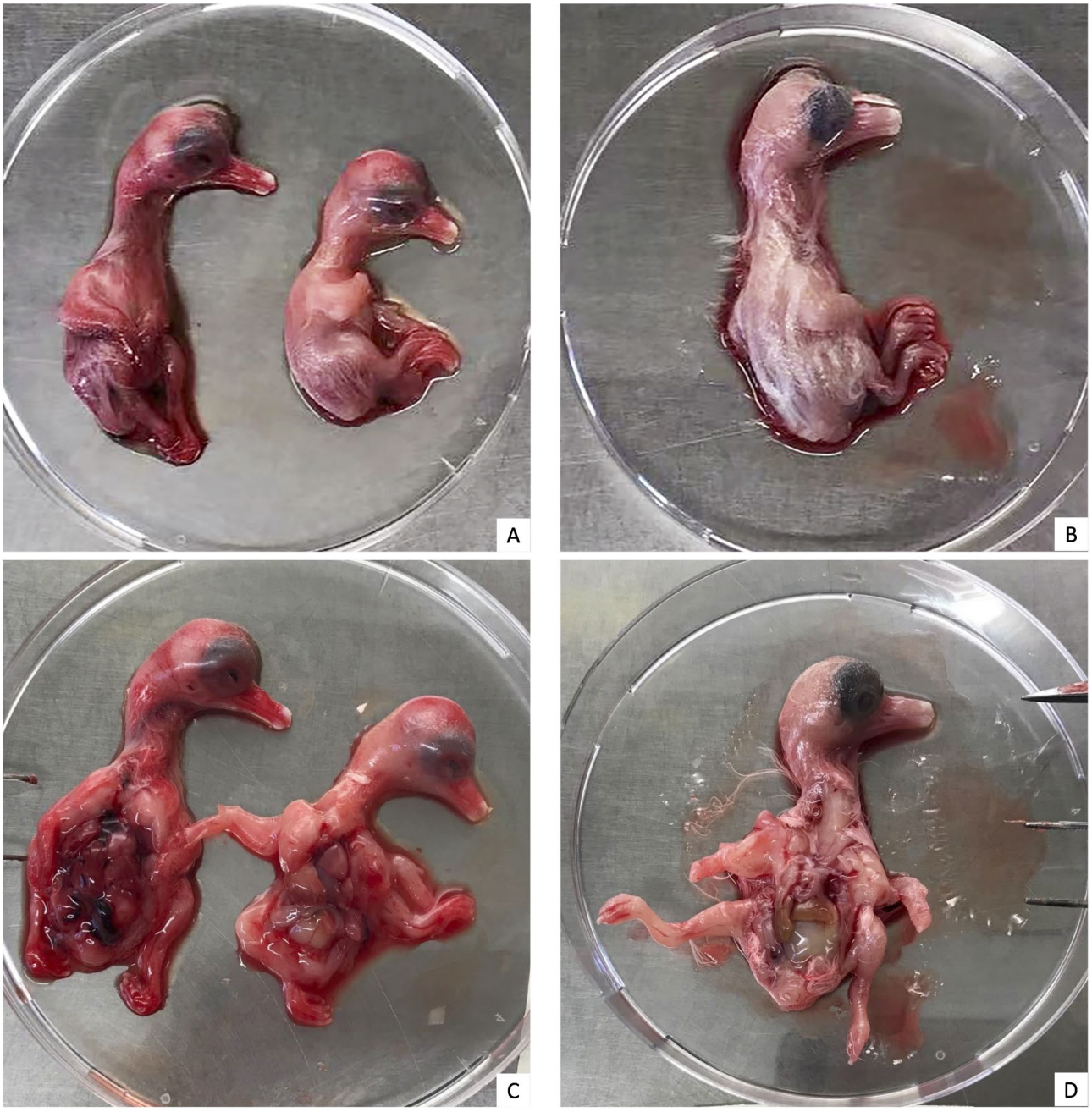


**Fig. 5** Effects of PiAdV-1 infection on pigeon embryo development. (**A & C**) Malformations and hyperemia in pigeon embryos with enlarged liver after inoculation with PiAdV-1 via yolk sac. (**B & D**) Normal development in phosphate-buffered saline-inoculated (control) pigeon embryos

detect pigeon pathogens; this method is widely used to identify infectious pathogenic microorganisms in laboratory and farm animals [38, 39]. mNGS revealed that the proportion of PiAdV-1 in each sample was highest (28240, 73138, 61819, 74205, 477841) and no other common pathogenic DNA viruses were detected in affected pigeons; these results corroborated the pathological diagnosis findings.

To date, the complete genome sequences available from pigeons were very limited: PiAdV-1 includes 2 strains (GenBank Accessions: NC_024474.1 and MW286325.1), and PiAdV-2 includes 1 strain (GenBank Accession: NC_031503.1). Whole genome sequencing of PiAdV-1 (P18-05523-6), isolated in 2018, revealed 99.3% sequence identity [9] to the PiAdV-1 reference strain (IDA4), which was isolated in 1995 [8]. This finding indicated that the sequence of PiAdV-1 has been highly conserved since its initial detection in the Netherlands in 1995. Sequencing analysis of the *hexon* gene suggested that the six PiAdV-1 isolates in the present study are closely related

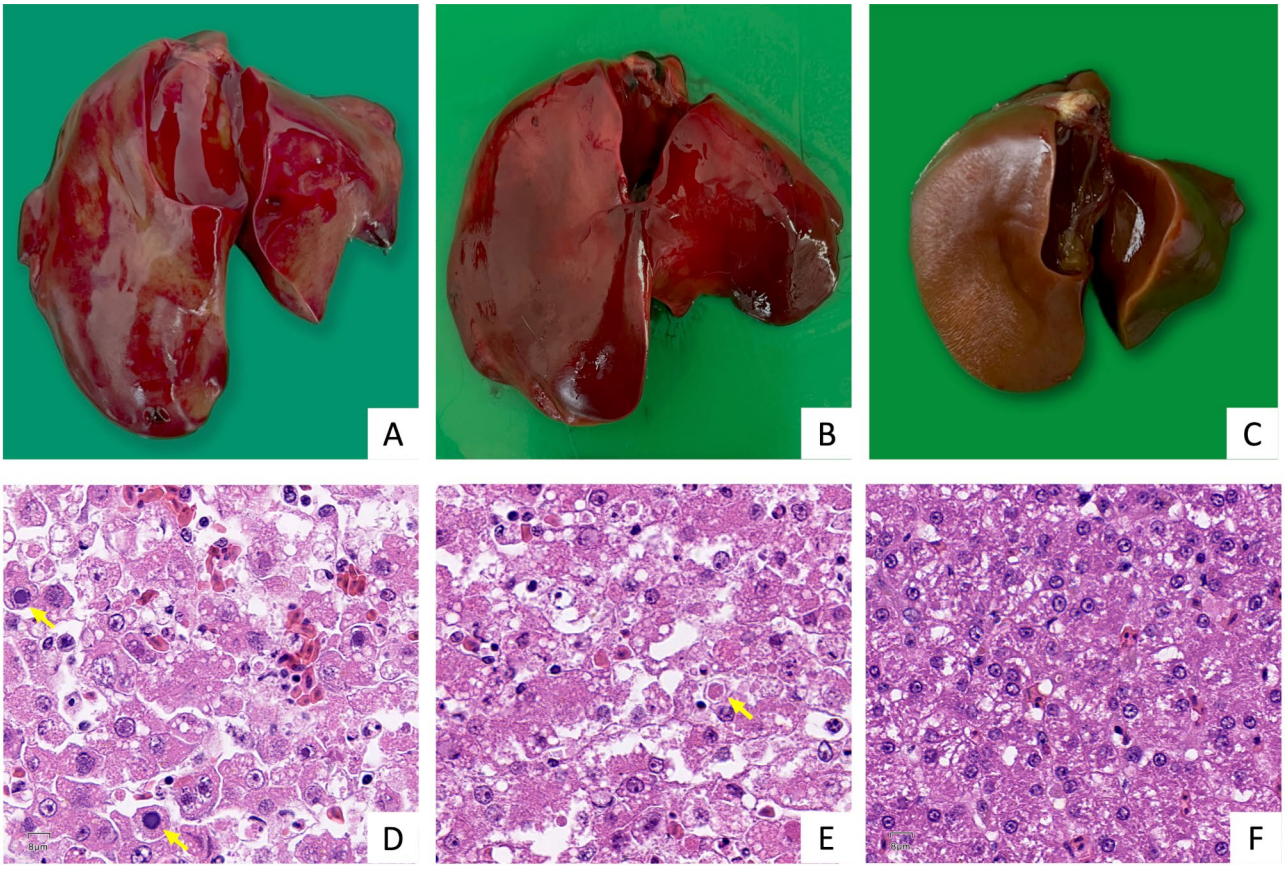


**Fig. 6** Pathological changes in the liver of pigeons inoculated with the isolate CH/BJ/1/2022. Significant liver enlargement and patchy hemorrhage in the liver were observed in the infected group (**A & B**), along with diffuse liver necrosis involving basophilic and eosinophilic inclusion bodies in hepatocyte nuclei (**D & E**). Pigeons in the control group exhibited normal liver morphology (**C & F**)

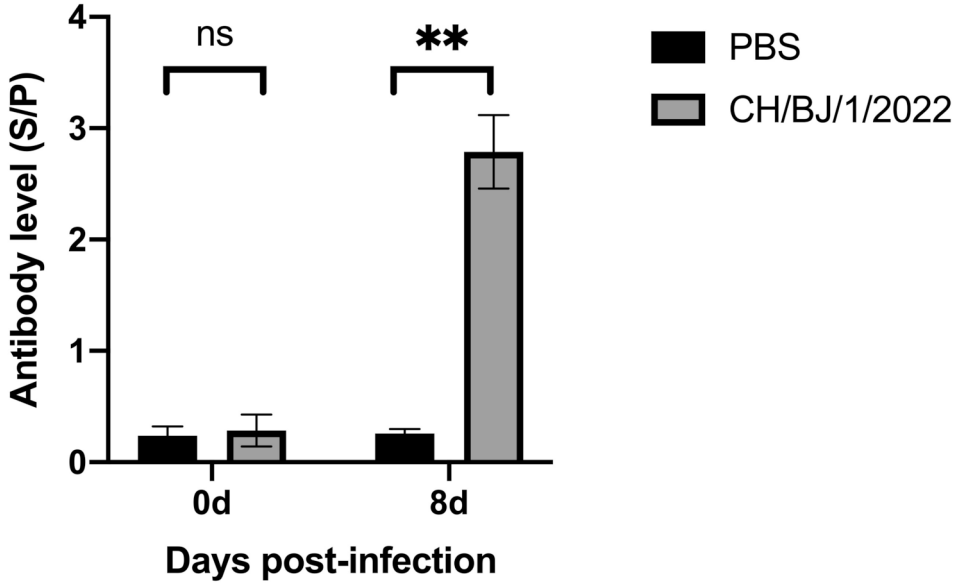


**Fig. 7** Serum antibody titers among infected pigeons at 8 dpi, **as determined by ELISA.** Asterisk indicates significant difference in antibody titer between the two groups. ns: $p \geq 0.05$, *: $p < 0.05$, **: $p < 0.01$

to P18-05523-6 (identified in Australia) and IDA4 (identified in the Netherlands) [9]. Additionally, upon comparison with both the IDA4 and P18-05523-6 strain, we found that the six PiAdV-1 isolates had a 10-amino acid deletion at residues 627–636 in the *fiber-2* gene and a 95-animo acid insertion at residue 75 in the 100 K gene (encoding hexon assembly protein 100 K). These structural variations may influence viral tropism, immune evasion, or replication efficiency, as fiber-2 is critical for host-cell receptor binding and 100 K plays an important role in transport of viral proteins during viral replication [40]. Globally, incomplete or unpublished genome sequences (e.g., TR/SKPA20 strain from Turkey and pAd-4 strain from Iran) hinder comprehensive analysis of fiber-2 and 100 K variations. Recently, PiAdV-1 strain isolated by Li et al. in China [27] also reported a 30-bp deletion in *fiber-2* gene compared to IDA4 strain but lacks precise positional annotation. They also highlighted sequence similarity to CH/BJ/1/2022, while the absence of full genomic data limits direct comparison of mutation profiles. Previous studies have indicated that a single amino acid mutation in the *hexon* gene or *fiber* gene make fowl adenovirus more virulent [41, 42]. Therefore, future studies should explore the functional implications of genetic variations on tissue tropism and immune evasion, as well as optimize cell culture systems for vaccine development against this emerging threat to pigeon industries.

Three strains of pigeon adenoviruses have been successfully isolated in chicken embryo liver cells [43, 44]; however, the isolation of pigeon adenoviruses in susceptible cells is difficult and not used as a standard diagnosis approach [7]. Although embryonated eggs are not suitable for use in the primary isolation of most aviadenoviruses, some FAdV isolates have demonstrated yolk sac or chorioallantoic membrane infection [33]. The successful isolation of virus in the present study indicated that embryonated pigeon eggs, which need to be confirmed negative for PiAdV antibodies, are susceptible to PiAdV-1 and could serve as the primary system for isolation of PiAdV-1. To confirm that PiAdV-1 was the etiological agent of the present infectious disease, we isolated the putative virus from infected birds and established a similar disease model by experimentally infecting normal healthy pigeons. These findings validate the pathogenicity of PiAdV-1 and highlight the urgent need for the prevention and control of PiAdV-1 in pigeon industry. Conventional poultry biosecurity measures prove insufficient due to unique pigeon husbandry: The "one-breeder-raises-Two/Three" practice in meat pigeons creates intensive parent-to-offspring transmission routes. Racing pigeon lofts aggregate birds from geographically dispersed sources, facilitating silent pathogen introduction via asymptomatic carriers. To address these challenges, vaccination is a cost-effective method for controlling pigeon adenovirus infections. Currently, no commercial vaccines are available for pigeon adenoviruses [45]. However, successful examples from fowl adenoviruses vaccines, such as the inactivated oil-emulsion FAdV-4 vaccine [46]and fiber-2 subunit vaccine [47], offer valuable insights for developing vaccines against pigeon adenoviruses.

## Conclusion

In conclusion, we isolated a new strain of PiAdV-1 from pigeons in Northern and Northwest China, and described the epidemiology, histopathology of the associated infection, as well as the genetic characteristics of the strain. Future studies regarding the origin and characteristics of this virus are needed to fully understand PiAdV and help to prevent its spread in China.

## Materials and methods

### Epidemiological investigation

Epidemiological data, including morbidity and mortality, were obtained by field investigators and through communication with local veterinarians at pigeon farms. Liver tissue and serum sample from naturally infected sick or deceased pigeons were obtained from local farms and racing pigeon organizing enterprises across seven provinces or cities in China, namely Beijing, Tianjin, Hebei, Shanxi, Shaanxi, Inner Mongolia, and Xinjiang(Fig. 8). Liver tissue samples were homogenized for PCR analysis and virus isolation, while serum samples were subjected to serological detection.

### Polymerase chain reaction (PCR) and electrophoresis

Liver tissue samples were homogenized in phosphate-buffered saline and centrifuged at 5000 rpm for 10 min. The supernatants were subjected to DNA extraction using the Takara MiniBEST Viral RNA/DNA Extraction Kit, version 5.0 (9766, Takara Bio), in accordance with the manufacturer's instructions. The extracted DNA samples were stored at -20°C until use. Primers specific for the *hexon* genes of pigeon adenovirus 1 (hexonA-F: 5'- CAACGTCACCACAGACAAGG-3' and hexonA-R: 5'- GTTTTCGCCTGTTCTTGACC-3'), pigeon adenovirus 2 (hexonB-F:5'-GTTTTCGCCTGTTCTTGACC-3' and hexonB-R: 5'- ACATATGTCGTCCCGCTCTC-3') and FAdV-C (hexonC-F:5'- GCAGGTAGAAAACGCC AACA-3' and hexonC-R: 5'- TGAACCCGATGTAGTT GGGC-3') were designed based on previous reports [8, 10, 48]. PCR was performed using Premix Taq™ Version 2.0 (R004A, Takara Bio, Japan), with the following thermocycler protocol: 30 cycles of denaturation at 98 °C for 10 s, annealing at 60 °C for 30 s, and extension at 72 °C for 30 s. PCR products were separated by 2.0% (w/v) agarose gel electrophoresis and photographed. The following


**Fig. 8** Distribution of sampled regions for PiAdV antibody and molecular detection, and locations of PiAdV presence in Northen and Northwest China

pathogens, including pigeon Newcastle disease virus (PiNDV) [49], pigeon herpesvirus (PiHV) [50], pigeon circovirus (PiCV) [26], *Chlamydia Psittaci* (*Cps*) [51], were detected using PCR or reverse transcription-PCR (RT-PCR).

### Serological test

Each blood sample was collected in Evacuated Blood Collection Tube (BD Vacutainer®, USA), and then was centrifuged at 4500 rpm for 10 min for serum separation. Antibodies against aviadenoviruses were measured using the Fowl Adenovirus Group 1 Antibody test kit (BioChek Ltd., The Netherlands), the microtiter plates of this kit have been pre-coated with inactivated FAdV antigen. In accordance with the manufacturer's instructions. Antibody titers were reported as sample-to-positive (S/P) ratios. Serum samples with S/P ratios of ≥0.5 were considered positive.

### Necropsy and histology

Necropsies were performed on sick and dead adult pigeons. Gross pathological findings were recorded and photographed. Tissue sections (e.g., liver, kidney, duodenum, jejunum, and heart) were fixed in 10% formalin. Routine hematoxylin and eosin staining was performed on tissue sections; lesions were observed via light microscopy and photographed.

### Transmission electron microscopy (TEM)

Liver specimens were cut into approximately 1-mm cubes, then fixed in 2.5% glutaraldehyde at 4 °C for 2 h. After tissues had been washed 3 times with phosphate buffer, they were immersed in 1% osmium tetroxide at 4 °C for 2 h. Subsequently, tissues were washed with sodium cacodylate buffer and dehydrated in an alcohol gradient; they were then placed in propylene oxide and embedded in Epon 812. Semithin Sect. (1 μm) were cut, stained with methylene blue, and localized under a microscope. Ultrathin sections were stained with uranyl acetate and lead citrate, then examined under a JEM-1400 transmission electron microscope. Photographs were acquired using a TEM-specific imaging system (charge-coupled device camera, 830.10U3, Gatan, USA).

### mNGS analysis of microorganism diversity in pericardial effusion

Pericardial effusion samples were collected from three sick adult pigeons and two sick young pigeons. Total genomic DNA was extracted using the Takara MiniBEST Viral RNA/DNA Extraction Kit, version 5.0 (9766, Takara Bio, Japan), in accordance with the manufacturer's instructions. The concentration and quality of the extracted DNA were determined using a Qubit Fluorometer (Thermo Fisher Scientific, USA) and gel electrophoresis. For mNGS, DNA libraries were constructed in accordance with the manufacturer's instructions (VAHTS

Universal DNA Library Prep Kit ND607), then sequenced on the Illumina NovaSeq 6000 platform (paired-end read length: 150 bp). Raw reads were filtered using Trimmomatic version 0.39 [52] and FastQC. Host reads were separated using the whole genome of *Columba livia* with bowtie2 [53] and samtools [54] softwares. The remaining reads were classified using kraken2 software [55] with standard RefSeq indexes, and the genomes of five common pigeon viruses were used for validation.

#### Sequence alignment and phylogenetic analysis

Specifically, all the positive samples for PiAdV-1 were subjected to PCR for sequencing and genome analysis of the *hexon* and *fiber-2* gene. Two pair of specific primers (hexon-F: 5'-TCGTGATCTCGCTCAGTGTC-3' and hexon-R: 5'-GGAAGGATTTGTCGAAGACG-3'; fiber-2-F: 5'-CGTCGACAGCTCAACTTCTG-3' and fiber-2-R: 5'-TCTCTGCCCGGTCTGTACTT-3') were designed. PCR was performed using PrimeSTAR® GXL DNA Polymerase (R050A, Takara Bio, Japan), with the following thermocycler protocol: 30 cycles of denaturation at 98 °C for 10 s, annealing at 60 °C for 15 s, and extension at 68 °C for 3 min 30 s (*hexon* gene) or 3 min (*fiber-2* gene), and a final extension at 68 °C for 2 min. PCR products were separated by agarose gel electrophoresis and photographed. The *fiber-2* and *hexon* genes of PiAdV-1 obtained in this study were subjected to phylogenetic analysis. Reference sequences of genus *Aviadenovirus* were retrieved from the NCBI nucleotide database. Phylogenetic trees were constructed using MEG7 (Molecular Evolutionary Genetics Analysis, version 7.0.26) with the neighbor-joining method, employing the Kimura 2-parameter model and bootstrap analysis with 1000 replicates. The resulting phylogenetic trees were visualized and annotated using Interactive Tree Of Life (iTOL) platform (https://itol.embl.de/).

#### Complete genome sequencing

Based on the available nucleotide sequence of PiAdV-1 (GenBank Accession: NC_024474.1), specific primers were designed to amplify the complete genome sequences of the virus isolated in this study, as shown in Table S1. All primers were synthetized by Sangon Biotech (Shanghai, China). Viral DNA from infected pigeon embryo homogenates were extracted using the Takara MiniBEST Viral RNA/DNA Extraction Kit, version 5.0 (9766, Takara Bio), following the manufacturer's instructions, and subsequently used for PCR amplification. PCR was performed using PrimeSTAR® GXL DNA Polymerase (R050A, Takara Bio, Japan), with the following thermocycler protocol: 30 cycles of denaturation at 98 °C for 10 s, annealing at 60 °C for 15 s, and extension at 68 °C for 3 min, and a final extension at 68 °C for 2 min. PCR products were examined by electrophoresis on a 1.0% (w/v) agarose gel, and those of the expected size were subjected to Sanger sequencing by Sangon Biotech (Shanghai, China). The complete sequences of PiAdV isolate were manually assembled and aligned with the PiAdV-1 reference sequence, IDA4 (GenBank Accession: NC_024474.1), to determine the nucleotide sequence homology using the Align Multiple DNA Sequences Tool in SnapGene software (version 6.0.2, www.snapgene.com).

#### Virus isolation

Liver tissues from dead pigeons with PCR-confirmed PiAdV-1 infection were homogenized and filtered through a 0.22-μm filter. The resulting supernatants were inoculated into the yolk sacs of PiAdV-free 6-day-old embryonated pigeon eggs and 6-day-old specific pathogen-free embryonated chicken eggs. All inoculated eggs were incubated at 37℃ for 10 days. Dead embryos were collected and immediately homogenized. Next, tissue homogenates were frozen and thawed twice; the clarified supernatants were filtered as described above, then subjected to three passages. Uninoculated embryos were included as negative controls. Successful virus isolation was regarded as the presence of viral infection with consistent embryo death and positive PCR detection.

#### Animal experiment

Ten 5-month-old Mirthys breeding pigeons were obtained from a breeding pigeon farm in Beijing, China. Enzyme-linked immunosorbent assays (BioChek Ltd., UK) showed that none of the pigeons carried antibodies to aviadenoviruses. Five pigeons were intramuscularly inoculated with 0.5 ml of virus (i.e., 1000 $ELD_{50}$ of CH/BJ/1/2022 isolate); the remaining five pigeons were injected with phosphate-buffered saline and served as a negative control group. The pigeons were housed in isolators. The investigators observed clinical signs at the same time each day. Serum samples were collected from all pigeons at 8 days post-inoculation (dpi) for ELISA-based antibody assessments. All pigeons were euthanized by inhalation of carbon dioxide at 8 dpi; liver tissue samples were collected for histopathological examination and virus isolation as described above.

#### Statistical analysis

Statistical analyses were performed by two-tailed t-tests using GraphPad Prism software (version 8.2.1 for Windows, GraphPad Software, USA). Statistical analyses were performed by two-tailed t-tests using GraphPad Prism software (version 8.2.1 for Windows, GraphPad Software, USA), with a 95% confidence interval set. Furthermore, all sample data were corrected to ensure the accuracy and reliability of the analysis results. *P* values of

<0.05 were considered statistically significant; *: $p < 0.05$, **: $p < 0.01$; ns: $p \geq 0.05$ [not significant].

**Abbreviations**

| | |
|---|---|
| PiAdV-1 | Pigeon adenovirus 1 |
| FAdV | Fowl adenoviruses |
| mNGS | Metagenomic next-generation sequencing |
| TEM | Transmission electron microscopy |
| $ELD_{50}$ | 50% embryo lethal dose |
| dpi | Days post-inoculation |
| PCR | Polymerase chain reaction |

## Supplementary Information

The online version contains supplementary material available at https://doi.org/10.1186/s12917-025-04724-w.

**Supplementary Material 1:** Supplementary Figure 1

**Supplementary Material 2:** Supplementary Figure 2

**Supplementary Material 3:** Supplementary Figure 3: Pathological features of PiAdV-1-infected pigeons. (**A-D**) Gross pathology: (**A**) Breast discoloration. (**B**) Renal enlargement. (**C**) Splenomegaly with patchy hemorrhage. (**D**) Hemorrhagic ovarian follicles. (**E-G**) Histopathology (H&E staining): (**E**) Pectoral muscle: Fibrous tissue lysis (arrows) and disorganized muscle fibers. (**F**) Kidney: Necrotic bile duct epithelium and inflammatory infiltration. (**G**) Liver: Vascular congestion and portal edema

**Supplementary Material 4**

**Acknowledgements**
We thank all farmers and veterinarians who assisted with sample collection. We thank professors Fenglong Wang, Zhenxuan Liu, Yi Jin, Lifeng Yang, and Jinling Wang for their help with histopathological analyses.

**Author contributions**
ZY, JL, and YL were responsible for study conception and design. ZY, YZ, JL, JG, WL, and YL collected samples. ZY, YZ, JL, HC, HD, and GW performed laboratory experiments. ZY, YZ, JL, JC, and JZ performed animal experiments. ZY, JL, and YL analyzed data. XW, JL, GL, SC, and YL provided intellectual input. SC and YL provided laboratory materials, reagents, and analysis tools. ZY, YZ, JL, XW, BL, and YL wrote and revised the manuscript. All authors reviewed and approved the final manuscript.

**Funding**
This study was funded by the Beijing Innovation Consortium of Agriculture Research System (BAIC06-2024-G10), a Science and technology innovation Project (KJCX20230213) from the Beijing Academy of Agricultural and Forestry Sciences, a Reform and Development Project (XMS202412) from the Institute of Animal Husbandry and Veterinary Medicine, Beijing Academy of Agricultural and Forestry Sciences, and a Youth Research Fund (QNJJ202234) from the Beijing Academy of Agricultural and Forestry Sciences.

**Data availability**
The datasets supporting the conclusions of this article are available from the corresponding author on reasonable request.

## Declarations

**Ethics approval and consent to participate**
Animal experiments in this study were approved by the Animal Welfare and Ethics Committee of the Institute of Animal Husbandry and Veterinary Medicine, Beijing Academy of Agriculture and Forestry Sciences (approval number: SYXK(Jing)2022-0003). All animal experiments were performed in strict accordance with the "Guidelines for Experimental Animals," established by the Ministry of Science and Technology (Beijing, China). All samples used in this study had obtained based on informed consent from farm owners.

**Competing interests**
The authors declare no competing interests.

Received: 7 October 2024 / Accepted: 28 March 2025
Published online: 14 April 2025

**References**

1. Marlier D, Vindevogel H. Viral infections in pigeons. Vet J. 2006;172(1):40–51.
2. Benko M, Aoki K, Arnberg N, Davison AJ, Echavarria M, Hess M, Jones MS, Kajan GL, Kajon AE, Mittal SK et al. ICTV virus taxonomy profile: adenoviridae 2022. J Gen Virol 2022, 103(3).
3. Griffin BD, Nagy E. Coding potential and transcript analysis of fowl adenovirus 4: insight into upstream ORFs as common sequence features in adenoviral transcripts. J Gen Virol. 2011;92(Pt 6):1260–72.
4. Russell WC. Adenoviruses: update on structure and function. J Gen Virol. 2009;90(Pt 1):1–20.
5. Harrach B, Tarjan ZL, Benko M. Adenoviruses across the animal Kingdom: a walk in the zoo. FEBS Lett. 2019;593(24):3660–73.
6. McFerran JB, McCracken RM, Connor TJ, Evans RT. Isolation of viruses from clinical outbreaks of inclusion body hepatitis. Avian Pathol. 1976;5(4):315–24.
7. Vereecken M, de Herdt P, Ducatelle R. Adenovirus infections in pigeons: A review. Avian Pathol. 1998;27(4):333–8.
8. Marek A, Kajan GL, Kosiol C, Harrach B, Schlotterer C, Hess M. Complete genome sequences of pigeon adenovirus 1 and Duck adenovirus 2 extend the number of species within the genus aviadenovirus. Virology 2014, 462–3:107–14.
9. Agnihotri K, Smith C, Oakey J, Storie G. Pigeon adenovirus and pigeon torque Teno virus associated with acute multifocal hepatic necrosis in pigeons in Queensland, Australia. Arch Virol. 2021;166(5):1469–75.
10. Teske L, Rubbenstroth D, Meixner M, Liere K, Bartels H, Rautenschlein S. Identification of a novel aviadenovirus, designated pigeon adenovirus 2 in domestic pigeons (Columba livia). Virus Res. 2017;227:15–22.
11. Wan C, Chen C, Cheng L, Shi S, Fu G, Liu R, Chen H, Fu Q, Huang Y. Detection of novel adenovirus in sick pigeons. J Vet Med Sci. 2018;80(6):1025–8.
12. McFerran JB, Smyth JA. Avian adenoviruses. Rev Sci Tech. 2000;19(2):589–601.
13. Hess M, Prusas C, Monreal G. Growth analysis of adenoviruses isolated from pigeons in chicken cells and serological characterization of the isolates. Avian Pathol. 1998;27(2):196–9.
14. Stenzel TA, Pestka D, Tykalowski B, Smialek M, Koncicki A. Epidemiological investigation of selected pigeon viral infections in Poland. Vet Rec. 2012;171(22):562.
15. Himmel L, O'Connor M, Premanandan C. Necrotizing hepatitis in a domestic pigeon (Columba livia). Vet Pathol. 2014;51(6):1171–3.
16. De Herdt P, Ducatelle R, Lepoudre C, Charlier G, Nauwynck H. An epidemic of fatal hepatic necrosis of viral origin in racing pigeons (Columba livia). Avian Pathol. 1995;24(3):475–83.
17. Chen S, Lin F, Jiang B, Xiao S, Jiang D, Lin C, Wang S, Cheng X, Zhu X, Dong H, et al. Isolation and characterization of a novel strain of Duck aviadenovirus B from muscovy Ducklings with acute hepatitis in China. Transbound Emerg Dis. 2022;69(5):2769–78.
18. Ye J, Liang G, Zhang J, Wang W, Song N, Wang P, Zheng W, Xie Q, Shao H, Wan Z, et al. Outbreaks of serotype 4 fowl adenovirus with novel genotype, China. Emerg Microbes Infect. 2016;5(5):e50.
19. Liu Y, Wan W, Gao D, Li Y, Yang X, Liu H, Yao H, Chen L, Wang C, Zhao J. Genetic characterization of novel fowl aviadenovirus 4 isolates from outbreaks of hepatitis-hydropericardium syndrome in broiler chickens in China. Emerg Microbes Infect. 2016;5(11):e117.
20. Kajan GL, Affranio I, Tothne Bistyak A, Kecskemeti S, Benko M. An emerging new fowl adenovirus genotype. Heliyon. 2019;5(5):e01732.
21. Schachner A, Matos M, Grafl B, Hess M. Fowl adenovirus-induced diseases and strategies for their control - a review on the current global situation. Avian Pathol. 2018;47(2):111–26.
22. Ketterer PJ, Timmins BJ, Prior HC, Dingle JG. Inclusion body hepatitis associated with an adenovirus in racing pigeons in Australia. Aust Vet J. 1992;69(4):90–1.
23. Zhuang Q, Wang S, Zhang F, Zhao C, Chen Q, Zhao R, Guo P, Ju L, Li J, Hou G, et al. Molecular epidemiology analysis of fowl adenovirus detected from apparently healthy birds in Eastern China. BMC Vet Res. 2023;19(1):5.

24. Sahindokuyucu I, Yazici Z, Barry G. A retrospective molecular investigation of selected pigeon viruses between 2018–2021 in Turkey. PLoS ONE. 2022;17(8):e0268052.
25. Ballmann MZ, Harrach B. Detection and partial genetic characterisation of novel avi- and siadenoviruses in racing and fancy pigeons (Columba Livia domestica). Acta Vet Hung. 2016;64(4):514–28.
26. Freick M, Muller H, Raue R. Rapid detection of pigeon herpesvirus, fowl adenovirus and pigeon circovirus in young racing pigeons by multiplex PCR. J Virol Methods. 2008;148(1–2):226–31.
27. Li Y, Wang J, Xiang C, Jing S, He H. Isolation of pigeon adenovirus 1 from dead pigeons with fulminant hepatitis course. Avian Dis. 2024;68(4):314–22.
28. Chen C, Zhu C, Chen Z, Cai G, Lin L, Zhang S, Jiang B, Miao Z, Fu G, Huang Y, et al. Rapid detection of pigeon adenovirus 2 using a TaqMan real-time PCR assay. Poult Sci. 2024;103(7):103848.
29. Rahimi Sardo E, Talazadeh F, Jafari RA, Seifi MR. Phylogenetic analysis of pigeon adenovirus 1 in clinical specimens of domestic pigeons (Columba Livia domestica) in Iran. Vet Res Forum. 2023;14(6):329–34.
30. Sahindokuyucu I, Turkmen MB, Sumer T, Elhag AE, Alcigir ME, Yazici Z, Barry G, Gulbahar MY, Kul O. First detection and molecular characterisation of a pigeon aviadenovirus A and pigeon circovirus co-infection associated with young pigeon disease syndrome (YPDS) in Turkish pigeons (Columba Livia domestica). Vet Med Sci. 2022;8(1):139–49.
31. Schachner A, Hess M. Special issue: avian adenoviruses. Viruses 2022, 14(4).
32. Hess M. Detection and differentiation of avian adenoviruses: a review. Avian Pathol. 2000;29(3):195–206.
33. El-Shall NA, El-Hamid HSA, Elkady MF, Ellakany HF, Elbestawy AR, Gado AR, Geneedy AM, Hasan ME, Jaremko M, Selim S, et al. Epidemiology, pathology, prevention, and control strategies of inclusion body hepatitis and hepatitis-hydropericardium syndrome in poultry: A comprehensive review. Front Vet Sci. 2022;9:963199.
34. Pereira FM, de Oliveira AR, Melo ES, Soares-Neto LL, Mangueira DK, Dos Santos DO, de Carvalho TP, Momo C, Santos RL. Naturally acquired infectious canine hepatitis in two captive maned Wolf (Chrysocyon brachyurus) puppies. J Comp Pathol. 2021;186:62–8.
35. Zhang Z, Lu C, Wang Y, Wang S, Dai D, Chen Z, Fan H. Molecular characterization and epidemiological investigation of pigeon circovirus isolated in Eastern China. J Vet Diagn Invest. 2011;23(4):665–72.
36. Saik JE, Weintraub ER, Diters RW, Egy MA. Pigeon herpesvirus: inclusion body hepatitis in a free-ranging pigeon. Avian Dis. 1986;30(2):426–9.
37. Abadie J, Nguyen F, Groizeleau C, Amenna N, Fernandez B, Guereaud C, Guigand L, Robart P, Lefebvre B, Wyers M. Pigeon circovirus infection: pathological observations and suggested pathogenesis. Avian Pathol. 2001;30(2):149–58.
38. Kwok KTT, Nieuwenhuijse DF, Phan MVT, Koopmans MPG. Virus metagenomics in farm animals: A systematic review. Viruses 2020, 12(1).
39. Han D, Li Z, Li R, Tan P, Zhang R, Li J. mNGS in clinical microbiology laboratories: on the road to maturity. Crit Rev Microbiol. 2019;45(5–6):668–85.
40. Shah MS, Ashraf A, Khan MI, Rahman M, Habib M, Chughtai MI, Qureshi JA. Fowl adenovirus: history, emergence, biology and development of a vaccine against hydropericardium syndrome. Arch Virol. 2017;162(7):1833–43.
41. Zhang Y, Liu A, Wang Y, Cui H, Gao Y, Qi X, Liu C, Zhang Y, Li K, Gao L, et al. A single amino acid at residue 188 of the Hexon protein is responsible for the pathogenicity of the emerging novel virus fowl adenovirus 4. J Virol. 2021;95(17):e0060321.
42. Pallister J, Wright PJ, Sheppard M. A single gene encoding the fiber is responsible for variations in virulence in the fowl adenoviruses. J Virol. 1996;70(8):5115–22.
43. Hess M, Prusas C, Vereecken M, De Herdt P. Isolation of fowl adenoviruses serotype 4 from pigeons with hepatic necrosis. Berl Munch Tierarztl Wochenschr. 1998;111(4):140–2.
44. Raue R, Hafez HM, Hess M. A fiber gene-based polymerase chain reaction for specific detection of pigeon adenovirus. Avian Pathol. 2002;31(1):95–9.
45. Santos HM, Tsai CY, Catulin GEM, Trangia KCG, Tayo LL, Liu HJ, Chuang KP. Common bacterial, viral, and parasitic diseases in pigeons (Columba livia): A review of diagnostic and treatment strategies. Vet Microbiol. 2020;247:108779.
46. Meng K, Yuan X, Yu J, Zhang Y, Ai W, Wang Y. Identification, Pathogenicity of Novel Fowl Adenovirus Serotype 4 SDJN0105 in Shandong, China and Immunoprotective Evaluation of the Newly Developed Inactivated Oil-emulsion FAdV-4 Vaccine. *Viruses.* 2019, 11(7).
47. Liu W, Liu M, Wang S, Tang Z, Liu J, Song S, Yan L. The development of a novel Fiber-2 subunit vaccine against fowl adenovirus serotype 4 formulated with oil adjuvants. Vaccines (Basel). 2024, 12(3).
48. Li HX, Wang J, Qiu LY, Han ZX, Liu SW. Fowl adenovirus species C serotype 4 is attributed to the emergence of hepatitis-hydropericardium syndrome in chickens in China. Infect Genet Evol. 2016;45:230–41.
49. Naveen KA, Singh SD, Kataria JM, Barathidasan R, Dhama K. Detection and differentiation of pigeon paramyxovirus serotype-1 (PPMV-1) isolates by RT-PCR and restriction enzyme analysis. Trop Anim Health Prod. 2013;45(5):1231–6.
50. Raue R, Schmidt V, Freick M, Reinhardt B, Johne R, Kamphausen L, Kaleta EF, Muller H, Krautwald-Junghanns ME. A disease complex associated with pigeon circovirus infection, young pigeon disease syndrome. Avian Pathol. 2005;34(5):418–25.
51. Hewinson RG, Griffiths PC, Bevan BJ, Kirwan SE, Field ME, Woodward MJ, Dawson M. Detection of chlamydia psittaci DNA in avian clinical samples by polymerase chain reaction. Vet Microbiol. 1997;54(2):155–66.
52. Bolger AM, Lohse M, Usadel B. Trimmomatic: a flexible trimmer for illumina sequence data. Bioinformatics. 2014;30(15):2114–20.
53. Langmead B, Salzberg SL. Fast gapped-read alignment with bowtie 2. Nat Methods. 2012;9(4):357–9.
54. Danecek P, Bonfield JK, Liddle J, Marshall J, Ohan V, Pollard MO, Whitwham A, Keane T, McCarthy SA, Davies RM et al. Twelve years of samtools and BCFtools. Gigascience 2021, 10(2).
55. Wood DE, Lu J, Langmead B. Improved metagenomic analysis with kraken 2. Genome Biol. 2019;20(1):257.


## Publisher's note